Journal of Cystic Fibrosis 21 (2022) 407–415

Contents lists available at ScienceDirect

Journal of Cystic Fibrosis

journal homepage: www.elsevier.com/locate/jcf

Original article

Needle-free iontophoresis-driven β-adrenergic sweat rate test

Audrey Reynaerts[a,e], François Vermeulen[b,f], Angélique Mottais[a,e], Sophie Gohy[b,e], Patrick Lebecque[b,e], Raphaël Frédérick[c,e], Rita Vanbever[d,e], Teresinha Leal[a,e,*]

[a] Louvain Center for Toxicology and Applied Pharmacology, Institut de Recherche Expérimentale et Clinique
[b] Cystic Fibrosis Center, Belgium
[c] Medicinal Chemistry Research Lab, Louvain Drug Research Institute
[d] Advanced Drug Delivery & Biomaterials, Louvain Drug Research Institute
[e] Université catholique de Louvain (UCLouvain), Brussels, Belgium
[f] Katholieke Universiteit Leuven (UZLeuven), Leuven, Belgium

ARTICLE INFO

Article history:
Received 21 April 2021
Revised 13 August 2021
Accepted 16 August 2021
Available online 4 September 2021

Keywords:
Cystic fibrosis
CFTR
Iontophoresis
Sweat gland
Sweat test
Nonlinear mixed-effects model

ABSTRACT

Objectives: Two CFTR-dependent β-adrenergic sweat rate tests applying intradermal drug injections were reported to better define diagnosis and efficacy of CFTR-directed therapies. The aim of this work was to develop and test a needle-free image-based test and to provide an accurate analysis of the responses.
Methods: The modified method was conducted by applying two successive iontophoresis sessions using the Macroduct device. Efficiency of drug delivery was tested by evaporimetry. Cholinergically stimulated sweating was evoked by pilocarpine iontophoresis. β-adrenergically stimulated sweating was obtained by iontophoresis of isoproterenol and aminophylline in the presence of atropine and ascorbic acid. A nonlinear mixed-effects (NLME) approach was applied to model volumes of sweat and subject-specific effects displaying inter- and intra-subject variability.
Results: Iontophoresis provided successful transdermal delivery of all drugs, including almost neutral isoproterenol and aminophylline. Pilocarpine was used at a concentration ~130-times lower than that used in the classical Gibson and Cooke sweat test. Addition of ascorbic acid lowered the pH of the solution, made it stable, prevented isoproterenol degradation and promoted drug iontophoresis. Maximal secretory capacity and kinetic rate of β-adrenergic responses were blunted in CF. A cutoff of 5.2 minutes for ET50, the time to reach the half maximal secretion, discriminated CF from controls with a 100% sensitivity and specificity. Heterozygous showed an apparently reduced kinetic rate and a preserved secretory capacity.
Conclusion: We tested a safe, well-tolerated needle-free image-based sweat test potentially applicable in children. Modelling responses by NLME allowed evaluating metrics of CFTR-dependent effects reflecting secretory capacity and kinetic rate.
© 2021 European Cystic Fibrosis Society. Published by Elsevier B.V. All rights reserved.

1. Introduction

Two sweat rate tests focusing on β-adrenergically regulated secretion have been reported to better define diagnosis, prognosis and efficacy of CFTR-directed therapies [1–3]. Their rationale is based on the dual control of regulation of sweating. The cholinergic control, regulated by calcium-activated chloride channels and mediated by muscarinic M3 receptors, predominates over the β-adrenergic control [4,5], that is CFTR-dependent, mediated by cAMP and defective in CF [5,6]. The preserved regulation of the cholinergic control in CF forms the basis of the classical Gibson and Cooke sweat test (GCST). Sharing similar pharmacological bases [1–3,6–13], the β-adrenergic tests differ in their outcome measures: in the image-based version [2,3,7–12], volumes of sweat droplets, termed bubbles, imaged at the surface of the skin during sweat secretion are measured; in the evaporimetry version [1,9], transepithelial water loss (TEWL) evaporated during sweat secretion is measured. Studies have shown that the image-based test is more sensitive to detect changes in secretion rates produced by CFTR modulator therapy [9]. Both tests resort to multiple intradermal drug injections, limiting their spreading among CF centers and making them less manageable in children. The use of multiple intradermal injections also reduces the applicability of the measurement as study endpoint. More recently, cholinergic stimulation of sweating, evoked by carbachol [1] or methacholine [2,3,7–9] injections, have been replaced by pilocarpine iontophoresis [10–12]. However, iontophoresis of aminophylline and isoproterenol, needed to maximize the β-adrenergic stimulation through intra-

* Corresponding author at: LTAP-IREC-UCLouvain, Avenue Hippocrate 57, BP-57.06; 1200 Brussels, Belgium.
E-mail address: Teresinha.leal@uclouvain.be (T. Leal).

https://doi.org/10.1016/j.jcf.2021.08.012
1569-1993/© 2021 European Cystic Fibrosis Society. Published by Elsevier B.V. All rights reserved.

cellular accumulation of cAMP, has been considered challenging and not reproducible [12,13]. The image-based test, considered as a ratiometric test [2,3,7–12], is analyzed by the ratio between β-adrenergically and cholinergically stimulated sweat secretion rates.

This work was designed to develop and test a needle-free version of the image-based β-adrenergic sweat test and to provide a more accurate data analysis modelling intra- and inter-subject variability of responses rather than calculating means of ratios of selected fractional slopes of rates of β-adrenergic and cholinergic responses. Parameters were estimated using the new method in a group of controls, CF and obligate carriers to assess diagnostic accuracy.

2. Materials and methods

The hospital-faculty ethics committees of UCLouvain and UZLeuven approved the study, registered as NCT03584841. Participating controls, patients with CF or heterozygous subjects read and signed inform consents. Controls were nonsmokers, had no self-reported indications of CF disease and no family history of CF. Patients had an established diagnosis of CF based on clinical manifestations, positive GCST (sweat chloride ≥60 mmol/L) and presence of two CF causing mutations. Heterozygous were parents of patients.

3. Clinical data

Age, sex, height and weight were collected from all tested subjects. Genetic screening was carried out by applying a mutation panel detecting the 71 most frequent European CFTR mutations (xTAG CF 71 Kit v2; Luminex Co®, Austin, TX, US). Comprehensive analysis of exons and intronic flanking regions of *CFTR* was performed by Dye Terminator Sequencing (v3.1/ABI 3130xl, Applied Biosystems®, Foster City, CA, US). CFTR databases 1 (http://www.genet.sickkids.on.ca/cftr/) and 2 (https://cftr2.org/) were used as references for information on individual mutations and their pathogenicity. Sweat chloride obtained by GCST, the presence of *Pseudomonas aeruginosa* infection, the status of pancreatic sufficiency and respiratory function were collected from electronic patient files. Patients with positive cultures of *P aeruginosa* in respiratory samples for at least six months with at least three positive cultures with one-month intervals between them were classified as colonized [14]. Pancreatic insufficiency was defined as fecal elastase <200 µg/g feces. Lung function, measured the day of the image-based test, was compared with a previous test performed 3-6 months earlier to confirm stability (<10% difference). Forced expiratory volume in 1 second (FEV_1) was expressed as percentage of predicted value for age, sex and height [15].

4. Iontophoresis instead of intradermal injections

The image-based test was performed by applying two successive iontophoresis sessions (1.5 mA for 5 minutes) at the same skin site using a Macroduct® 3700 device (ELITechGroup; Brussels, Belgium). Drugs infused in felt pads (3 mm thickness) were applied at the anode and NaCl 0.9% at the cathode. As for the GCST, the electrodes were placed at the inner volar surface of a forearm halfway between the elbow and the wrist [16]. The efficiency of drug iontophoresis was tested by evaporimetry [1]. Following iontophoresis, the stimulated skin area, cleaned with 70% alcohol, was coated with a thin layer of a corpitolinol-enriched oil emulsion (Laboratoires Urgo, Chenôve, France). The evaporimeter (CyberDerm RG-1; Broomall, PA, US) measuring probe was secured on the skin site of the anode.

To select the pilocarpine concentration, concentration-dependent TEWL effects were examined using pilocarpine concentrations ranging from 2.6×10^{-5} to 2.6×10^{-3} M. Atropine was tested at a concentration (740×10^{-6} M) ~5-times higher than that used for pilocarpine. The efficiency of skin delivery of isoproterenol and aminophylline was evaluated after iontophoresing the cAMP-elevating agents at concentrations used in previous studies [13,17,18] (Supplementary Table S1).

5. Image record and analysis

After iontophoresis, a Plexiglas circular well (2.27 cm^2) was secured over the stimulated skin area (6.37 cm^2). The bottom of the well was filled with a thin layer of unstained or erioglaucine blue-stained water-saturated mineral oil, as previously described [2]. Images of bubbles formed under the oil layer were recorded for 10 or 30 minutes during the cholinergic or the β-adrenergic phases respectively. The optical setup consisted in a digital Nikon (Japan) D7100 camera fitted with a Nikkor 105mm macro lens and a kit of four Nikon Asservi R1 flashes, mounted in a Kaiser RS2 CP camera stand (Germany) and coupled to a monitor for live view mode. It was connected to a timer remote control TC-252-DC2 (Nikon) allowing automatic recording of images at 30 second intervals. Manual image analysis was done using the Image J software (https://imagej.nih.gov/ij/) [2,3,7–11].

6. Drugs

All drugs were obtained at a pharmacopoeia grade. Pilocarpine nitrate salt and isoproterenol hydrochloride were purchased from Sigma–Aldrich (Overijse, Belgium), aminophylline and ascorbic acid from ACA Pharma (Nazareth, Belgium), and atropine sulfate from Sterop Pharmaceutical (Brussels, Belgium). Erioglaucine disodium salt (CAS No. 3844-45-9) was purchased from Fisher Scientific (Merelbeke, Belgium) and mineral oil (CAS No. 8042-47-5) from Sigma-Aldrich. Solutions were used within 4 hours after preparation. Pilocarpine solution was prepared in water. The ready-for-use atropine solution for clinical applications (Sterop Pharmaceutical) served as a solvent for aminophylline, isoproterenol and ascorbic acid powder.

7. Statistical analysis

Descriptive statistical analysis was performed using the JMP Pro 11 software (SAS Institute, Cary, NC, US). Prior to statistical analysis, data were checked for normality (Shapiro-Wilk normality test). In cases of skewed distributions of continuous variables, medians were chosen as measures of centrality and between-group comparisons were made by Wilcoxon rank test with Bonferroni adjustment. Analysis of sweat volumes was carried out by a nonlinear mixed-effects (NLME) model [19] using a specially designed R script (available on request). The NLME approach was fitted using a sigmoid Emax model involving the following parameters: maximum effect Emax; time to reach the half maximum effect, ET50; and sigmoidicity factor gamma which controls the nonlinearity of the model through the curvature reflected in the steepness of the growth curve [19]. By applying the Hill equation [20], individual parameters estimated by subject and by phase allowed between-group comparisons and receiver operating curve (ROC) analysis. The null hypothesis was rejected at $p<0.05$.

8. Results

8.1. Successful drug iontophoresis

To evaluate the efficiency of drug delivery by iontophoresis, a total of 27 TEWL assays were performed in 8 controls (Table 1),

Table 1
Anthropometric, clinical and laboratory data of subjects tested during protocol development tests by evaporimetry (pretest) and during the image-based β-adrenergic (test) studies
ID: subject identity; V: controls tested during protocol development tests by evaporimetry; Control (CTRL), CF or heterozygous (HTZ) subjects tested during the image-based β-adrenergic test. F: female, M: male. Y: yes; N: no. PA: *Pseudomonas aeruginosa* colonization; PI: pancreatic insufficiency; PS: pancreatic sufficiency. Legacy names used for mutation nomenclature. *: newly identified CFTR mutation, not reported in CFTR database 1 or 2. HTZ3: non-genotyped mother of a child displaying an F508del/N1303K genotype. Values expressed as means (SE).

ID	Genotype	Age years	Sex F/M	BMI kg/cm^2	Sweat Cl mmol/L	FEV1%pred	Pancreatic status PS/PI	PA N/Y
V1		29	F	38.3				
V2		29	F	19.8				
V3		34	F	31.3				
V4		24	F	26.3				
V5		26	M	24.3				
V6		73	M	21.3				
V7		25	F	20.2				
V8		65	F	20.8				
		38.1 (15.4)	6/8	25.3 (5.0)				
CTLR1		72	M	21.6				
CTLR2		20	M	19.7				
CTLR3		19	M	21.7				
CTLR4		30	F	21.2				
CTLR6		35	F	18.0				
CTLR8		31	F	22.2				
CTLR9		28	M	32.9				
CTLR10		30	F	17.8				
		33.1 (16.6)	4/4	21.9 (4.7)				
HTZ1	1717-1G>A	50	M	25.1				
HTZ2	F508del	35	F	22.0				
HTZ3	F508del or N1303K	36	F	18.1				
HTZ4	F508del	46	M	23.8				
HTZ5	F508del	41	M	30.1				
HTZ6	F508del	48	F	23.7				
HTZ7	F508del	47	M	26.5				
		43.3 (5.9)	3/4	24.2 (3.7)				
CF1	F508del/G542X	31	M	20.9	118	29	PI	Y
CF2	F508del/F508del	38	M	20.9	98	42	PI	Y
CF3	F508del/306insA	29	M	20.5	104	64	PI	Y
CF7	F508del/F508del	34	F	18.0	120	32	PI	Y
CF8	F508del/ 1717-1G>A	21	F	19.5	120	93	PI	N
CF10	Q890X/I105A>T *	56	F	22.9	76	51	PS	Y
CF14	G542X/R553X	18	M	16.7	78	68	PI	Y
CF15	F508del/I507del	39	F	20.3	95	56	PI	Y
		33.3 (11.8)	4/4	20.0 (1.9)	101 (17.8)	54.4 (21.0)	1/7	1/7

tested at a 4- to 7-day interval. TEWL values recorded after pilocarpine iontophoresis showed a concentration-dependent saturation effect (Fig. 1A). To avoid possible contamination of the subsequent phase, the 140 $\times$ 10^{-6} M submaximal pilocarpine concentration (Fig. 1A) and a ~5-times higher atropine concentration were selected. Fig. 1B shows a representative TEWL tracing obtained after iontophoresing pilocarpine at the selected concentration. The efficiency of atropine transdermal flow was demonstrated by the blockage of pilocarpine responses after iontophoresing the inhibitor (Fig. 1C) and was confirmed by prevention of the cholinergic effect when atropine preceded pilocarpine (Fig. 1D). The pH of pilocarpine solution, stable for 1 month at room temperature [16], was 7.5. That of atropine solution, stable at room temperature for 18 months [21], was 4.2. Aminophylline and isoproterenol were tested at 23.8 $\times$ 10^{-3} M and 32.4 $\times$ 10^{-3} M [13,17,18] respectively. The basic (pH 8.4) solution containing atropine and the cAMP-elevating agents did not provide consistent and reproducible responses. Moreover, it was unstable with a strong ocher color developing soon after its preparation (Supplementary Figure S1A). Protecting it from light exposure did not prevent degradation (Supplementary Figure S1B). Sequential addition of the drugs to the ready-for-use atropine solution identified isoproterenol as responsible for the change. Adding 0.22 M ascorbic acid to prevent oxidation [22,23] provided a stable solution with a lowered pH (3.4; Supplementary Figure S2A,B, Supplementary Table S2) and efficient transdermal drug delivery with repeatable TEWL results. Fig. 1E illustrates a representative TEWL tracing including three iontophoretic sessions. Mean TEWL values are shown in Fig. 1F. Protocol development tests were well tolerated and no iontophoresis-related burns were observed.

8.2. Data population for the β-adrenergic test

Patients with CF, tested under stable conditions, were not enrolled in other clinical trials or under CFTR modulator therapy. Anthropometric and clinical data are shown in Table 1. P aeruginosa colonization was absent in one patient. All but one were pancreatic insufficient. The genotype associated with pancreatic suffi-

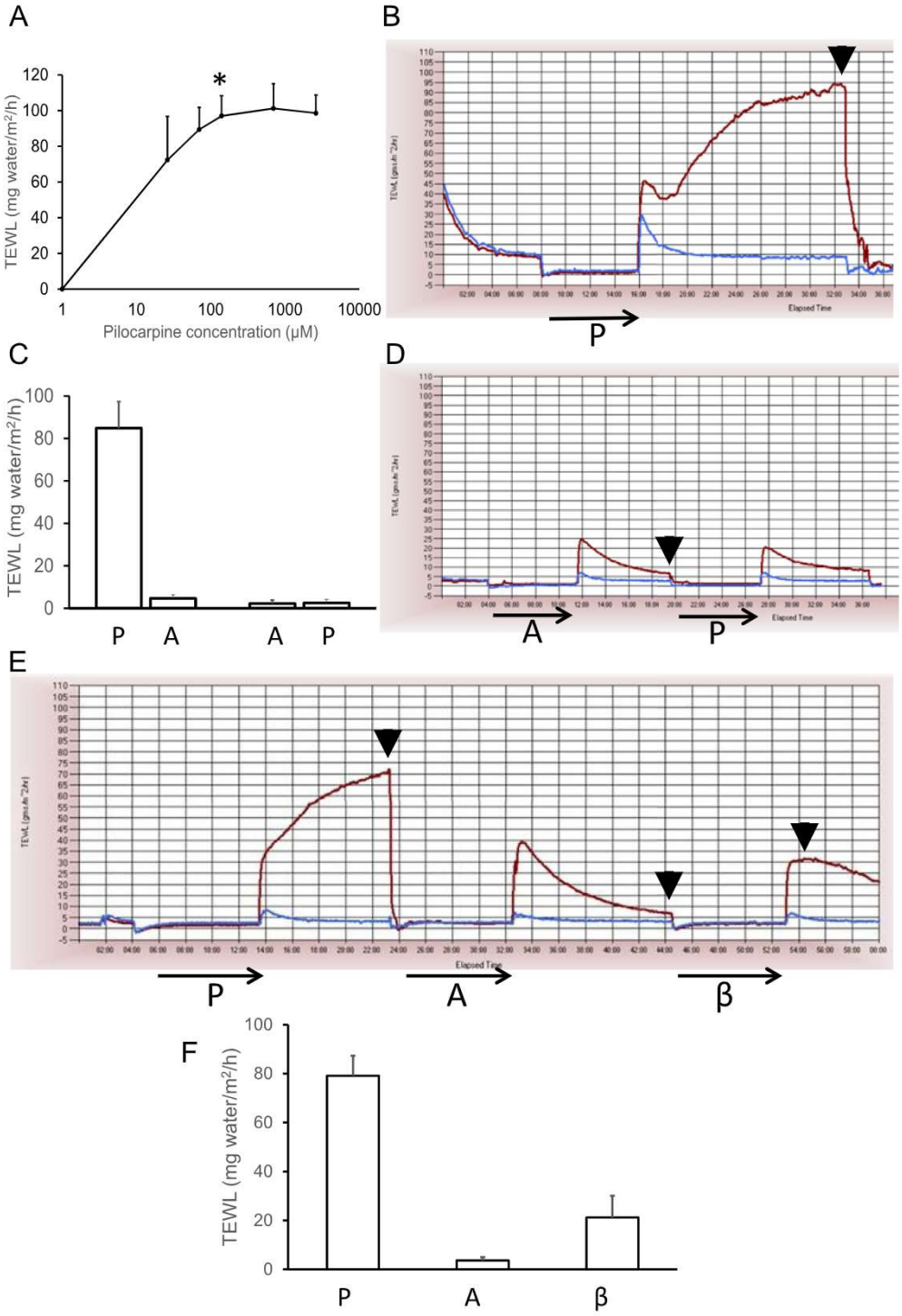

Fig. 1. Transepithelial water loss (TEWL, mg of water/m²/h) measurements to evaluate efficiency of transdermal delivery of pilocarpine, atropine, aminophylline and isoproterenol by iontophoresis. Efficiency of drug delivery through the skin expressed as the TEWL value (mg of water/m²/h) recorded at the end of the stimulation of sweating with pilocarpine or β-adrenergic (atropine + aminophylline + isoproterenol) plus ascorbic acid) or the inhibition of sweating with atropine. TEWL values were corrected by subtracting the background transpiration rate recorded at the reference probe (blue line) at the same corresponding time. (A) Concentration-dependent effect of pilocarpine iontophoresis analyzed from a total of 27 tests performed in 8 healthy subjects (3-5 tests per subject) with different drug concentrations, at a 4- to 7-day intervals between tests. The mean (± SE) TEWL value obtained under the submaximal 140 × 10^{-6} M pilocarpine concentration (*), selected for further studies, was 97 (± 11.3) mg of water/m²/h. (B) Screen copy of a representative TEWL tracing obtained after iontophoresing pilocarpine at the selected concentration. The arrowhead indicates the time of the maximal TEWL value. (C) TEWL values showing blockage of the pilocarpine response when atropine was followed by pilocarpine (left bars, P-A; n: 5), and prevention of pilocarpine response when atropine was preceded by pilocarpine (right bars, A-P; n: 6). (D) Screen copy of a representative TEWL tracing obtained after atropine iontophoresis performed before pilocarpine iontophoresis showing prevention of pilocarpine response. The arrowheads indicate the time of the representative TEWL values. (E) Screen copy of a representative TEWL tracing obtained after iontophoresis of a solution containing atropine, the cAMP-elevating agents (aminophylline + isoproterenol) and ascorbic acid, preceded by iontophoresis of pilocarpine iontophoresis and of atropine. The arrowheads indicate the time of the representative TEWL values (maximum for pilocarpine response, minimum for atropine response and maximum for β-adrenergic response). (F) TEWL values obtained after iontophoresis/electroosmosis of cAMP-elevating agents (aminophylline + isoproterenol) plus ascorbic acid solution preceded by pilocarpine and atropine in 5 subjects. Arrows indicate the duration of iontophoresis including cleaning the skin area and placement of evaporimeter probes. P: 140 × 10^{-6} M pilocarpine solution. A: 740 × 10^{-6} M atropine solution. β: β-adrenergic (23.8 × 10^{-3} M aminophylline + 32.4 × 10^{-3} M isoproterenol) plus 0.22 M ascorbic acid solution.

ciency was I105A>T, not reported in CFTR databases. The new variant transforms T in A at position 446 and destroys a restriction site at a highly conserved region of exon 4. It was detected in a female (CF10) displaying a Q890X mutation in trans, diagnosed at 28 years with mild respiratory symptoms and 76 mmol/L sweat chloride.

8.3. Sweat bubbles induced by drug iontophoresis

We first determined if we could identify bubble formation and growth following iontophoresis. The procedure flow, the setup and illustrative images of the test, lasting about 55 minutes, are illustrated in Fig. 2A-I. The optical setup (Fig. 2E) allowed capture of high resolution (6,000 × 4,000 pixels) images with improved sharpness and increased depth of field (Fig. 2F-I). Bubble growth kinetics of the β-adrenergic phase in controls (Fig. 2G) confirmed the efficiency of iontophoresis to deliver the cAMP-elevating agents. The diameter of bubbles formed at the end of the β-adrenergic phase (Fig. 2G) appeared to be similar to that originally reported in injection-driven tests [2,3].

8.4. Confirmation of β-adrenergic responses blunted in CF and apparently reduced in heterozygous

Representative tracings of bubble volumes obtained in a control, a heterozygous and a patient are illustrated in Fig. 3A-C. Values from 23 tests (8 healthy, 8 CF and 7 heterozygous), representing 2,593 curves of kinetics of bubble growth from a total of 11,604 observations, are depicted in Fig. 3D. As distributions were not normal, medians or log-scaled values are shown. Individual subject curves are shown in Supplementary Figures S3-4. Pilocarpine (P)-curves did not differ between groups (Fig. 3A-C). However, shallower β-adrenergic (β)-curves were observed in CF (Fig. 3C). In line with previous studies [2,3,6–12], an apparently intermediate pattern of β-responses was observed in heterozygous (Fig. 3B).

8.5. Goodness of fit of the NLME model

Rather than calculating means of individual ratios of the selected maximal fractional slopes of the β-adrenergic and cholinergic responses, we applied a NLME approach allowing integrating observable variables, termed fixed effects, and unobservable variables, termed random effects [19]. Fixed effects allowed estimating parameters of volume of bubbles by phase and by group [20]. Random effects accounted for inter-individual (n:23), inter-phase (n:2) and inter-bubble variability (n:60 for each subject except for subject CF10 for whom 30 bubbles were mapped and processed for analysis). Accurate goodness of fit plots of the NLME model is shown in Supplementary Figure S5.

8.6. ET50 of β-curves as the most discriminating parameter

No significant between-group differences for the parameter estimates of P-responses were noticed. Accordingly, NLME analysis using Emax of P-phase, meaning the maximum sweat volume after pilocarpine stimulation at a plateau obtained when integrating volume responses of all bubbles per group, per phase and per subject, as a fixed effect did not show significant differences between CF or heterozygous and controls (p values 0.60 or 0.70, respectively). However, when fitting Emax of β-responses of the control group as a reference, we found significantly reduced Emax, ET50 and gamma in CF (Fig. 4A-C, individual parameter values are shown in Supplementary Table S3). The most discriminating parameter with no overlap between CF and non-CF was ET50. An apparently lower gamma median value (Fig. 4C) was observed in heterozygous (1.27) relative to controls (1.66), however the difference did not reach significance (p:0.09; Wilcoxon test with Bonferroni adjustment).

8.7. Sensitivity and specificity

Sensitivity, specificity, cutoff value and area under the ROC curve performed for the β-parameters are summarized in Fig. 4D. Again, ET50 was the most accurate parameter discriminating CF from controls. An ET50 cutoff of 5.2 minutes, providing a 100% sensitivity and specificity, and an area under the ROC curve of 1.0, discriminated the two groups. A similar ET50 cutoff value discriminated CF from heterozygous. Heterozygous were discriminated from controls with a 100% sensitivity for Emax and ET50 but with a low specificity (25% and 37.5% respectively). Gamma provided the highest specificity (43.9%) to discriminate heterozygous from controls. In line with a large heterogeneity of β-responses in controls, cutoff values of Emax (87.8 nL) and/or ET50 (10.8 min), and/or a cutoff value of gamma (1.6) would be required to discriminate heterozygous from controls.

9. Discussion

The present study was designed to develop and test a non-invasive version of the image-based β-adrenergic sweat test and to provide an adequate analysis of repeated longitudinal measurement data obtained during the tests. With regard to the non-invasiveness of the test, we based ourselves on the physicochemical drug properties to promote their transdermal iontophoretic delivery (Supplementary Table S4) and on electroosmosis, an additional iontophoretic mechanism that can assist skin permeation of neutral drugs [24–26]. With regard to a more appropriate data analysis, we applied a NLME approach, a well-suited model for kinetic analysis of repeated measurement data modelling together observable variables and a subset of subject-specific effects displaying inter- and intra-subject variability [19].

We report here successful results of needle-free image-based tests in CF, heterozygous and controls while applying two iontophoresis sessions using the most standardized, fully automated, accredited iontophoretic power source without increasing iontophoretic current or duration [13]. Forming the basis of iontophoresis of positively charged pilocarpine during the GCST [16], iontophoresis has many practical advantages: it is safe with no adverse events except of few reports of burns [16]. The method has been used for other applications such as local anesthesia of positively charged lidocaine and/or epinephrine in children, with comfort and minimal inter-subject variability [27].

To avoid contamination of the subsequent β-adrenergic phase, pilocarpine was iontophorised at a concentration ~130 times lower than that present in Pilogel® discs and ~260 times lower than that used by others [12,13,18] and atropine was applied at a ~5-times higher concentration than that used for pilocarpine. Iontophoresis of the cAMP-elevating agents, needed to maximize the β-adrenergic stimulation through intracellular accumulation of cAMP, has been reported as being challenging and non-reproducible [12,13]. The fact that iontophoresis conventionally involves flow of charged molecules across the skin can explain, at least partly, unsuccessful trials with isoproterenol (or salbutamol) and aminophylline iontophoresis [12,13]. Pharmacologically incompatible when mixed together for iontophoresis studies, aminophylline was documented to promote isoproterenol degradation [12]. Isoproterenol is a synthetic catechol compound devoid of acid/base properties in aqueous solution (Supplementary Table S4). Moreover, susceptible to oxidation, the two catechol groups present in the isoproterenol molecule polymerize to form orthoquinones, responsible for the ocher color changes observed in fresh solutions. Likely resulting in skin toxicity that may evoke immune responses [28], conversion to orthoquinones should be prevented. Adding ascorbic acid as a reducing agent [22,23] resulted in a solution stable for at least 48 hours of a pH close to that of the

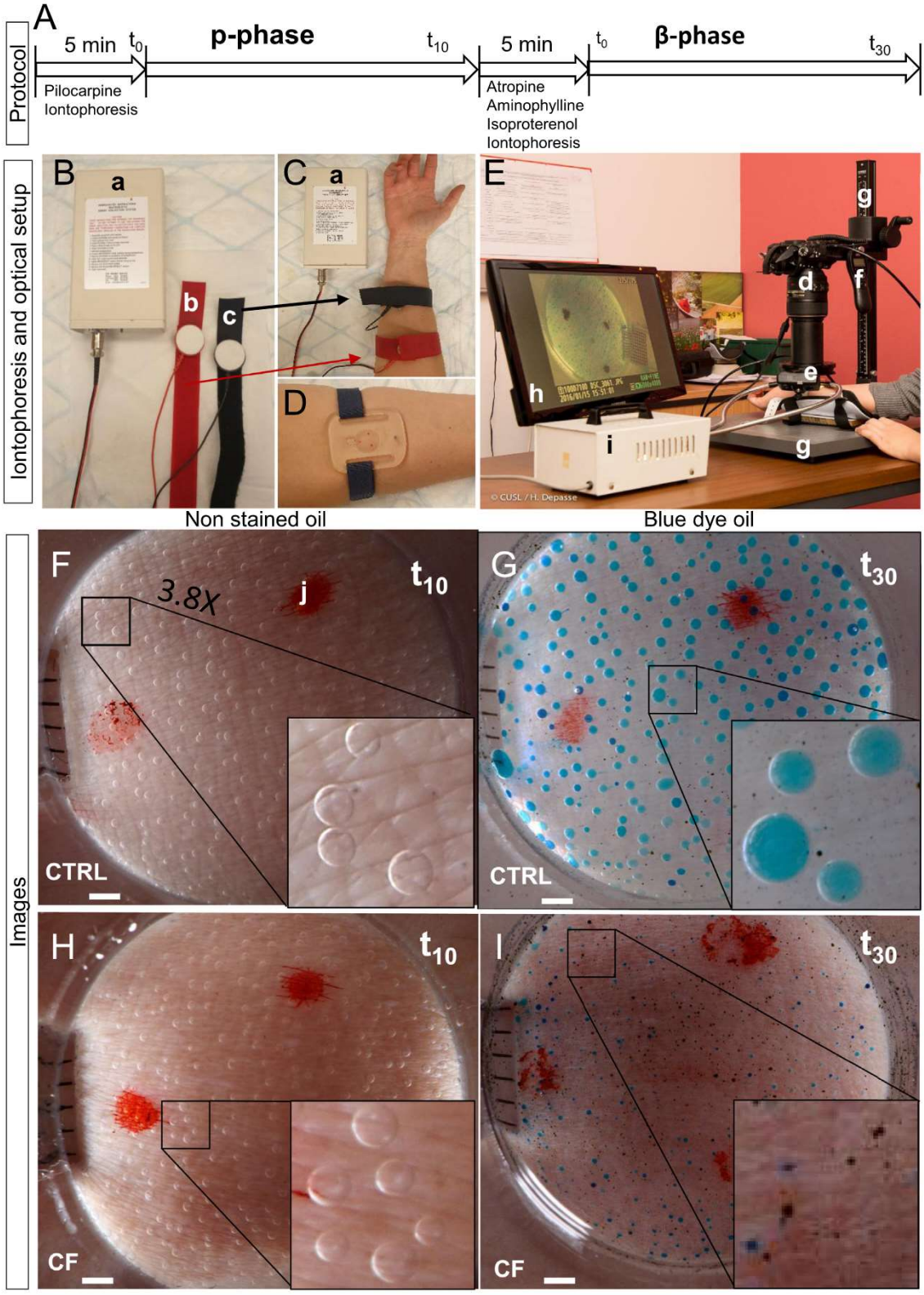

Fig. 2. Procedure flow, iontophoresis and optical setup, and illustrative images obtained during the image-based β-adrenergic test. (A) Iontophoresis of pilocarpine was followed by capture of serial images for 10 minutes (p-phase), then by a second iontophoresis, applied at the same skin site, of a solution containing atropine, aminophylline and isoproterenol *plus* ascorbic acid followed by recording images for 30 minutes (β-phase). The whole duration of the test was about 55 minutes. (B) Macroduct® 3700 (a) used for iontophoresis. Felt pads (3 mm thickness) soaked with drugs were fitted inside the circular of the Macroduct® anode (b) and with saline placed at the cathode (c). (C) Electrodes fixed onto a forearm of the subject following the international recommendations for the classical GCST. (D) Plexiglas circular well (2.27 cm^2) placed at the stimulated skin area (anode) and filled with a thin layer of unstained or erioglaucine blue-stained water-saturated mineral oil. (E) Optical setup comprising a digital camera fitted with a macro lens (d), a kit of four rosette-shaped flashes (e), a timer remote control for automatic recording of serial images (f), mounted in a camera stand (g) and coupled to a monitor for live view mode (h). Swan neck white light (i). Images of sweat bubbles formed under the oil layer recorded at 10 minutes of the p-phase in a control (F) and in a patient with CF (G) and at 30 minutes of the β-phase in a control (H) and in a patient with CF (I). In panel F, (j) is one of the marks used to align successive images. Calibration bar: 1 mm. Inserts in panels E-H magnified 3.8x. (For interpretation of the references to color in this figure legend, the reader is referred to the web version of this article.)

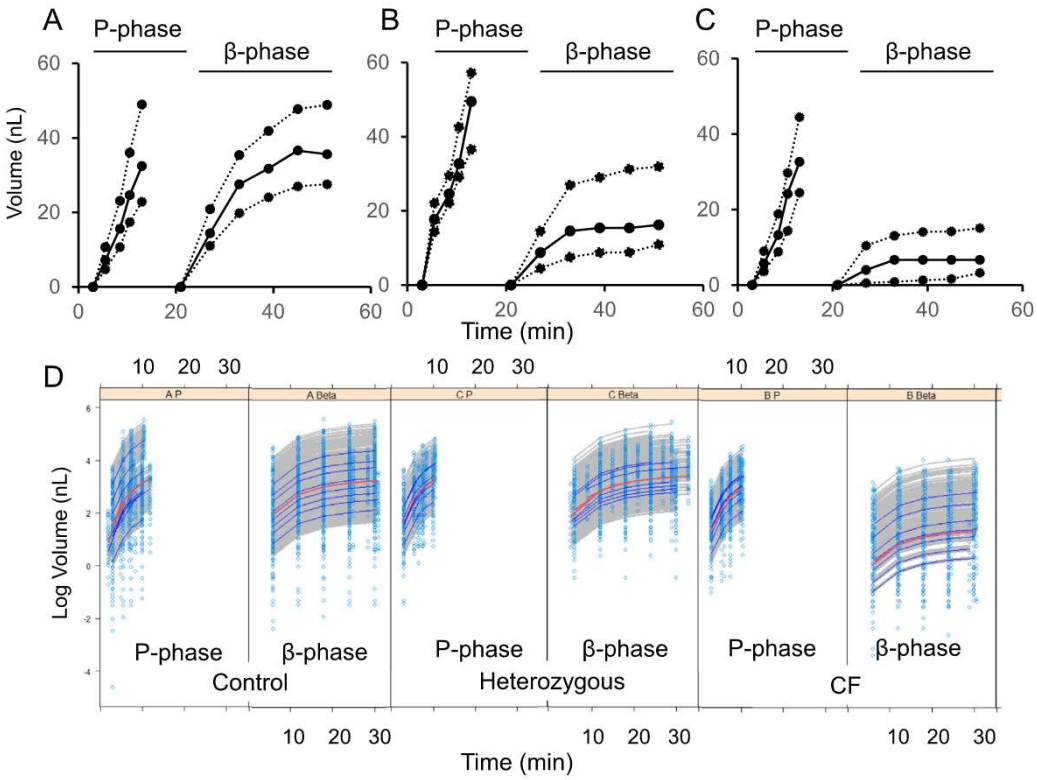

Fig. 3. Representative tracings of sweat volumes as a function of time and of test phase in a control (A), a heterozygous (B) and a patient with CF (C). Nonlinear mixed-effects model fit of sweat volumes plotted as log-scaled data for the 23 tested subjects (D). Sweat volumes obtained from CTRL1 control (A), HTZ7 heterozygous subject (B) and CF2 patient with CF (C) after pilocarpine iontophoresis (P-phase) followed by iontophoresis of a solution containing atropine, cAMP-elevating drugs and ascorbic acid (β-phase). As they did not follow a normal distribution, values were plotted as median (solid line), 75th and 25th percentiles (upper and lower dashed lines). (D) Sweat volumes obtained during the P-phase and the β-phase from 8 controls, 7 heterozygous and 8 patients with CF. Grey lines represent individual bubble fitted curves; blue lines represent individual subject medians; red lines represent population medians, and dots represent individual observed values. (For interpretation of the references to color in this figure legend, the reader is referred to the web version of this article.)

skin (~4). Converted into a highly positively charged compound at a low pH, isoproterenol became iontophoresable by ion flow during the electric stimulus. The efficacy of iontophoresis of positively charged atropine was also improved by lowering the pH of the solution. Atropine contains a tertiary amine group (Supplementary Table S4) fully protonated at such a low pH. We showed here that iontophoresis of atropine at a concentration ~5 times higher than that used for pilocarpine fully inhibited or prevented pilocarpine effect. This is in line with previous studies [29] showing that an even lower 1:10 atropine:pilocarpine molar ratio abolishes the cholinergic effect of pilocarpine. Aminophylline is the ethylenediamine salt of theophylline. Ethylenediamine has two protonable amine functions while theophylline is an almost neutral compound. Lowering the pH of the solution to a value closer to that of the pKa(base) of aminophylline (2.44) increased the proportion of positively charged theophylline molecules, thus favoring its anodal iontophoresis. Iontophoretic mechanisms involved in transdermal delivery of aminophylline probably included a combination of increased current-related ion flow and associated electroosmotic flow of solvent. Electroosmosis has been applied to promote user-friendly transdermal delivery of insulin, commonly administered by subcutaneous injection [30].

NLME models are new sophisticated regression techniques developed in the early 1990's now increasingly used for pharmacokinetic analysis [19] and in distinct other fields. As an example, NLME approaches have been used in forest data analysis to quantify and predict volumes of Eucalyptus trees by modelling multilevel mixed effects [31]. In our study, applying an NLME approach allowed confirming functional integrity of cholinergic control of sweating and refractoriness to β-adrenergic stimulation in CF. β-responses reflecting secretory capacity and kinetic rate were blunted in CF. The most discriminating parameter was ET50 with a cutoff of 5.2 minutes fully discriminating CF from controls (or heterozygous). Our findings suggested that the secretion rate in response to β-adrenergic stimulation tends to be reduced in heterozygous and that secretory capacity is preserved. Discriminating heterozygous from a control population required a combination of accuracy of prediction by parameters, gamma being the one with the highest specificity. Analyzing the three parameters (Emax, ET50 and gamma) generated by NLME analysis, which integrates multiple random effects on top of fixed effects, would contribute to improve the correspondence between observations and prediction.

10. Conclusion

In this work, we succeeded for the first time in performing a needle-free, fully iontophoresis-driven version of the image-based β-adrenergic sweat test, thus making it noninvasive, well tolerated, manageable in children and also applicable to the evaporimetry test. By integrating inter- and intra-subject variability, modelling test responses by NLME allowed evaluating metrics of CFTR-dependent effects reflecting secretory capacity and kinetic rate. We showed here that all CFTR-dependent parameters are blunted in CF while heterozygous have an apparently lowered kinetic rate and a preserved secretory capacity. Our findings shed some light on accuracy of prediction of biomarkers, with potentiality in pediatrics, crucially needed for CF drug development. The new version of the test we developed hold promise for its validation by other CF centers and its large application to study drug effects and pharmacodynamics in clinical trials with CFTR modulators, in particular in

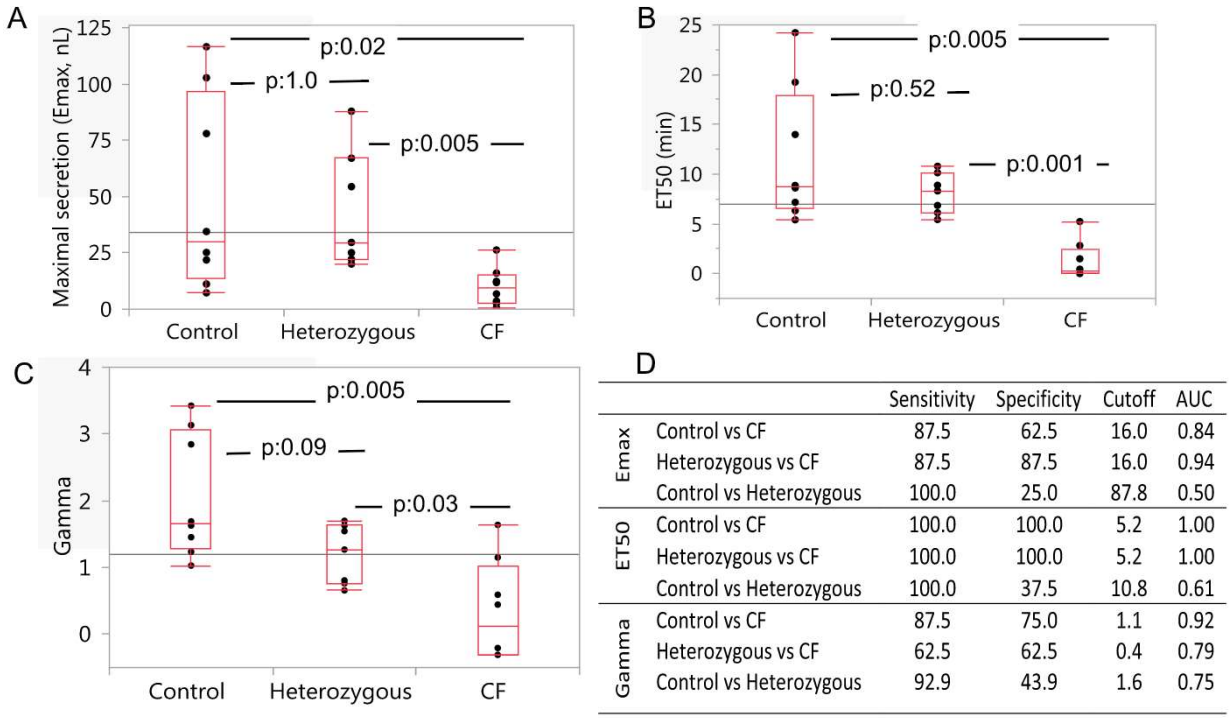

D

		Sensitivity	Specificity	Cutoff	AUC
Emax	Control vs CF	87.5	62.5	16.0	0.84
	Heterozygous vs CF	87.5	87.5	16.0	0.94
	Control vs Heterozygous	100.0	25.0	87.8	0.50
ET50	Control vs CF	100.0	100.0	5.2	1.00
	Heterozygous vs CF	100.0	100.0	5.2	1.00
	Control vs Heterozygous	100.0	37.5	10.8	0.61
Gamma	Control vs CF	87.5	75.0	1.1	0.92
	Heterozygous vs CF	62.5	62.5	0.4	0.79
	Control vs Heterozygous	92.9	43.9	1.6	0.75

Fig. 4. Distributions and between-group comparisons of parameter estimates of the β-phase and their accuracy for prediction by ROC analyses. Box plots of parameter estimates of β-responses from controls, heterozygous and CF groups following nonlinear mixed-effects analyses (A-C). Analyses were modelled by using Emax of the β-response of the control group as fixed effect and parameters were estimated by the Hill equation. (A) Emax, expressed as nL per gland, corresponds to the maximal sweat volume. (B) ET50, expressed in minutes, corresponds to the time of half maximum effect. No overlapping value between CF and non-CF groups was shown for ET50: the lowest value in the control or in the heterozygous group was 5.40 or 5.42 minutes respectively; the highest value in the CF group was 5.22 minutes. (C) Gamma, a dimensionless sigmoidicity factor, controls the nonlinearity of the model through the curvature reflected in the steepness of the growth curve. Horizontal lines of box plots illustrate the 0.5th, 25th, 50th (median), 75th and 99.5th percentiles of the corresponding parameter (A-C). The horizontal line across each panel (A-C) represents the mean of the whole study group. p values obtained from between-group comparisons of medians made by Wilcoxon test with Bonferroni adjustment are reported (A-C). (D) Sensitivity, specificity, cutoff value and area under the ROC curve for each of the Hill parameters of β-responses.

pediatric cohorts or prediction of prognosis from a positive newborn screening result. To this aim, improving the optical set up consisting in a high image resolution miniature device allowing user-friendly movements of the arm without disturbing alignment of serial images would make the test even easier and comfortable for application in infants.

Disclosure

Part of the study has been presented at the 42nd European Cystic Fibrosis Conference, held 5-8 June 2019, Liverpool, United Kingdom [abstract WS04-3] and at the Virtual 43rd European Cystic Fibrosis Conference, held 24-25 September 2020 [abstract WS09.2].

Declaration of Competing Interest

None.

CRediT authorship contribution statement

Audrey Reynaerts: Investigation, Visualization, Data curation, Writing – original draft. **François Vermeulen:** Investigation. **Angélique Mottais:** Investigation. **Sophie Gohy:** Investigation. **Patrick Lebecque:** Investigation. **Raphaël Frédérick:** Methodology. **Rita Vanbever:** Methodology. **Teresinha Leal:** Conceptualization, Supervision, Validation, Project administration, Writing – review & editing.

Acknowledgments

We are indebted to all volunteers tested during the study. The study was supported by the Belgian CF Foundation Association Muco. The authors thank Professor J. Lebacq for critically editing the manuscript, Jan Feijer (Galapagos, The Netherlands) for contributing to the initial discussion on the data analysis, Céline Bugli (Statistical Methodology and Computing Service (SMCS), Louvain Institute of Data Analysis and Modelling in economics and statistics (LIDAM), Louvain-la-Neuve, Belgium) for final statistical analysis, Thao Nguyen Khoa (Centre de Référence Maladies Rares: Mucoviscidose et affections liées à CFTR, Université de Paris, France) for training in the evaporimetry test and Paola Melotti (CF center, Azienda Ospedaliera Universitaria Integrata Verona, Italy) for support through the study. Rita Vanbever is Research Director of the Fonds National de la Recherche Scientifique (Belgium).

Supplementary materials

Supplementary material associated with this article can be found, in the online version, at doi:10.1016/j.jcf.2021.08.012.

References

[1] Quinton P, Molyneux L, Ip W, Dupuis A, Avolio J, Tullis E, Conrad D, Shamsuddin AK, Durie P, Gonska T. β-adrenergic sweat secretion as a diagnostic test for cystic fibrosis. Am J Respir Crit Care Med 2012;186(8):732–9. doi:10.1164/rccm.201205-0922OC.

[2] Wine JJ, Char JE, Chen J, Cho HJ, Dunn C, Frisbee E, Joo NS, Milla C, Modlin SE, Park IH, Thomas EAC, Tran KV, Verma R, Wolfe MH. In vivo readout of CFTR function: ratiometric measurement of CFTR-dependent secretion by individual, identifiable human sweat glands. PLoS One 2013;8(10):e77114 10.1371/journal.pone.0077114. eCollection 2013.

[3] Char JE, Wolfe MH, Cho HJ, Park IH, Jeong JH, Frisbee E, Dunn C, Davies Z, Milla C, Moss RB, Thomas EA, Wine JJ. A little CFTR goes a long way: CFTR-dependent sweat secretion from G551D and R117H-5T cystic fibrosis subjects taking ivacaftor. PLoS One 2014;9(2):e88564 eCollection 2014. doi:10.1371/journal.pone.0088564.
[4] Sato K. The physiology, pharmacology, and biochemistry of the eccrine sweat gland. Rev Physiol Biochem Pharmacol 1977;79:51–131. doi:10.1007/BFb0037089.
[5] Sato K, Sato F. Defective beta adrenergic response of cystic fibrosis sweat glands in vivo and in vitro. J Clin Invest 1984;73(6):1763–71. doi:10.1172/JCI111385.
[6] Behm JK, Hagiwara G, Lewiston NJ, Quinton PM, Wine JJ. Hyposecretion of beta-adrenergically induced sweating in cystic fibrosis heterozygotes. Pediatr Res 1987;22(3):271–6. doi:10.1203/00006450-198709000-00007.
[7] Bergamini G, Tridello G, Calcaterra E, Ceri S, Tagliasacchi M, Bianchi F, Monti F, Masciadri A, Laudanna E, Peserico D, Sorio E, Esposito V, Leal T, Assael BM, Sorio C, Melotti P. Ratiometric sweat secretion optical test in cystic fibrosis, carriers and healthy subjects. J Cyst Fibros 2018;17(2) 186-19. doi:10.1016/j.jcf.2017.12.003.
[8] Treggiari D, Kleinfelder K, Bertini M, Tridello G, Fedrigo A, Pintani E, Iansa P, Casiraghi A, Minghetti P, Cipolli M, Sorio C, Melotti P. Optical measurements of sweat for in vivo quantification of CFTR function in individual sweat glands. J Cyst Fibros 2021 S1569-1993(21)00052-7. doi:10.1016/j.jcf.2021.03.003.
[9] Kim J, Farahmand M, Dunn C, Davies Z, Frisbee E, Milla C, Wine JJ. Evaporimeter and bubble-imaging measures of sweat gland secretion rates. PLoS One 2016;11(10):e0165254 eCollection 2016. doi:10.1371/journal.pone.0165254.
[10] Reynaerts A, Melotti P, Vermeulen F, Gohy S, Lebecque P, Leal T. WS04-3 A non-invasive version of the beta-sweat test. J Cyst Fibros 2019;18(S1):S7.
[11] Reynaerts A, Vermeulen F, Melotti P, Gohy S, Frédérick R, Nietert M, Leal T. Automated image analysis of cystic fibrosis transmembrane conductance regulation-dependent, b-adrenergic-evoked sweat secretion driven by iontophoresis. J Cyst Fibros 2020;19(S2):S15.
[12] Salinas DB, Peng YH, Horwich B, Wee CP, Frisbee E, Maarek JM. Image-based β-adrenergic sweat rate assay captures minimal cystic fibrosis transmembrane conductance regulator function. Pediatr Res 2020;87(1):137–45. doi:10.1038/s41390-019-0503-8.
[13] Shamsuddin AKM, Reddy MM, Quinton PM. Iontophoretic beta-adrenergic stimulation of human sweat glands: possible assay for cystic fibrosis transmembrane conductance regulator activity in vivo. Exp Physiol 2008;93(8):969–81. doi:10.1113/expphysiol.2008.042283.
[14] Döring G, Conway SP, Heijerman HG, Hodson ME, Høiby N, Smyth A, et al. Antibiotic therapy against pseudomonas aeruginosa in cystic fibrosis: a European consensus. Eur Respir J 2000;16(4):749–67 Ocdoi: 10.1034/j.1399-3003.2000.16d30.x.
[15] Stanojevic S, Bilton D, McDonald A, Stocks J, Aurora P, Prasad A, Cole TJ, Davies G. Global Lung Function Initiative equations improve interpretation of FEV1 decline among patients with cystic fibrosis. Eur Respir J 2015;46(1):262–4. doi:10.1183/09031936.00187314.
[16] C.L.S.I. Sweat testing specimen collection and quantitative chloride analysis. CLSI guideline C34. 4th ed. Wayne, PA: Clinical and Laboratory Standards Institute; 2019.
[17] Buono MJ, Gonzalez G, Guest S, Hare A, Numan T, Tabor B, White A. The role of in vivo beta-adrenergic stimulation on sweat production during exercise. Auton Neurosci 2010 Jun 24;155(1-2):91–3. doi:10.1016/j.autneu.2009.12.006.
[18] Gonska T, Ip W, Turner D, Han WS, Rose J, Durie P, Quinton P. Sweat gland bioelectrics differ in cystic fibrosis: a new concept for potential diagnosis and assessment of CFTR function in cystic fibrosis. Thorax 2009;64(11):932–8. doi:10.1136/thx.2009.115295.
[19] Fine KL, Grimm KJ. Examination of nonlinear and functional mixed-effects models with nonparametrically generated data. Multivariate Behav Res 2020;22:1–18 10.1080/00273171.2020.1754746.
[20] Goutelle S, Maurin M, Rougier F, Barbaut X, Bourguignon L, Ducher M, Maire P. The Hill equation: a review of its capabilities in pharmacological modelling. Fundam Clin Pharmacol 2008;22(6):633–48. doi:10.1111/j.1472-8206.2008.00633.x.
[21] Jira T, Pohloudek-Fabini R. [Analysis and stability of atropine sulfate and scopolamine hydrobromide. 3: studies on the stability of tropane alkaloids; 80: contribution to problems in the use of plastic containers for liquid pharmaceuticals]. Pharmazie 1983;38(8):520–3 PMID: 6634922.
[22] Smith G, Hasson K, Clements JA. Effects of ascorbic acid and disodium edetate on the stability of isoprenaline hydrochloride injection. J Clin Hosp Pharm 1984;9(3):209–15. doi:10.1111/j.1365-2710.1984.tb01078.x.
[23] Nayak AS, Cutie AJ, Jochsberger T, Kay AI. The effect of various additives on the stability of isoproterenol hydrochloride solutions. Drug Dev Ind Pharm 1986;12(4):589–601 doi.org/10.3109/03639048609048031.
[24] Pikal MJ. The role of electroosmotic flow in transdermal iontophoresis. Adv Drug Deliv Rev 2001;46(1-3):281–305. doi:10.1016/s0169-409x(00)00138-1.
[25] Tokumoto S, Mori K, Higo N, Sugibayashi K. Effect of electroporation on the electroosmosis across hairless mouse skin in vitro. J Control Release 2005;105(3):296–304. doi:10.1016/j.jconrel.2005.04.002.
[26] Pliquett UF, Gusbeth CA, Weaver JC. Non-linearity of molecular transport through human skin due to electric stimulus. J Control Release 2000;68(3):373–86. doi:10.1016/s0168-3659(00)00271-6.
[27] DeCou JM, Abrams RS, Hammond JH, Lowder LR, Gauderer MW. Iontophoresis: a needle-free, electrical system of local anesthesia delivery for pediatric surgical office procedures. J Pediatr Surg 1999;34(6):946–9. doi:10.1016/s0022-3468(99)90765-0.
[28] Bolton JL, Dunlap TL, Dietz BM. Formation and biological targets of botanical o-quinones. Food Chem Toxicol 2018;120:700–7. doi:10.1016/j.fct.2018.07.050.
[29] Wang H, Shi H, Lu Y, Yang B, Wang Z. Pilocarpine modulates the cellular electrical properties of mammalian hearts by activating a cardiac M3 receptor and a K+ current. Br. J. Pharmacol. 1999;126(8):1725–34. doi:10.1038/sj.bjp.0702486.
[30] Ahad A, Raish M, Bin Jardan YA, Al-Mohizea AM, Al-Jenoobi FI. Delivery of insulin via skin route for the management of diabetes mellitus: approaches for breaching the obstacles. Pharmaceutics 2021;13(1):100. doi:10.3390/pharmaceutics13010100.
[31] Dantas D, Calegario N, Junior F, Carvalho S, Junior M, Melo E. Multilevel nonlinear mixed-effects model and machine learning for predicting the volume of Eucalyptus spp. trees. Cerne 2020;26(1):48–57. Retrieved from http://www.cerne.ufla.br/site/index.php/CERNE/article/view/2286 .